

Optical modifications of polymers by ion beam irradiation*

C. Darraud†, B. Bennamane, C. Gagnadre, J. L. Decossas and J. C. Vareille
*Laboratoire d'Electronique des Polymères sous Faisceaux Ioniques, Faculté des Sciences,
 123 Avenue Albert Thomas, 87060 Limoges Cedex, France
 (Received 23 September 1993; revised 12 November 1993)*

Polymers subjected to ion beam or γ irradiation undergo structural modifications, which lead to an increase in refractive index for some materials, such as poly(diethylene glycol bis(allyl carbonate)) (CR39) and polycarbonate. The refractive index variation achieved with ion beam irradiation is sufficient to produce optical waveguides in CR39. The waveguide losses have been systematically studied in order to apply this technique to integrated optics (microstructure fabrication). A fundamental study using various spectroscopic methods (i.r. and u.v.-visible) has also been carried out, with the aim of gaining a better understanding of the structural modifications of polymeric materials caused by irradiation.

(Keywords: optical waveguides; ion beam irradiation; structural modifications)

INTRODUCTION

Exposure of polymeric materials, such as poly(diethylene glycol bis(allyl carbonate)) (CR39), polycarbonate and poly(bisphenol A bis(allyl carbonate)) (HIRI), to γ rays or ion beam irradiation leads to modification of their refractive index¹. The refractive index, n , increases with increasing γ irradiation dose. In the case of ion beam irradiation, the change depends on the kind of ions, their energy and the fluence (number of ions per cm²); the refractive index variation ($\Delta n = n_{\text{after irradiation}} - n_{\text{before irradiation}}$) is sufficient to produce optical waveguides²⁻⁴.

Our aim is to control the performance of these waveguides by increasing our understanding of the various physical and chemical processes induced by irradiation⁵. Several methods of investigation are used, such as gel permeation chromatography (g.p.c.), i.r. spectroscopy and u.v.-visible spectroscopy, which show that degradation is the main irradiation-induced process.

EXPERIMENTAL

Materials

CR39 was prepared by bulk polymerization of the liquid monomer allyl carbonate ester of diethylene glycol. Allylcarbonate ester of Bisphenol A was polymerized to yield HIRI. These two polymers have the repeat units shown in Figures 1a and b, respectively. Both materials are thermosets cured with peroxides as initiators. Peroxides dissociate in the liquid monomer into radicals which initiate polymerization. Two initiators are commonly used: diisopropyl peroxydicarbonate and dicyclohexyl peroxydicarbonate.

A common polycarbonate produced by Bayer Industry was used. Its formula is shown in Figure 2.

* Presented at 'Physical Aspects of Polymer Science — Polymer Physics Group 16th Biennial Meeting', 15–17 September 1993, University of Reading, UK

† To whom correspondence should be addressed

Irradiation

An HVEE 400 kV accelerator was used to irradiate the material with H, He, Li and B ions, with energies between 50 and 300 keV and fluences ranging from 10¹³ to 5 × 10¹⁵ ions cm⁻².

A ⁶⁰Co source delivering a dose rate of 3 × 10³ Gy h⁻¹ was used for the γ irradiation, with doses ranging from 60 to 2000 kGy.

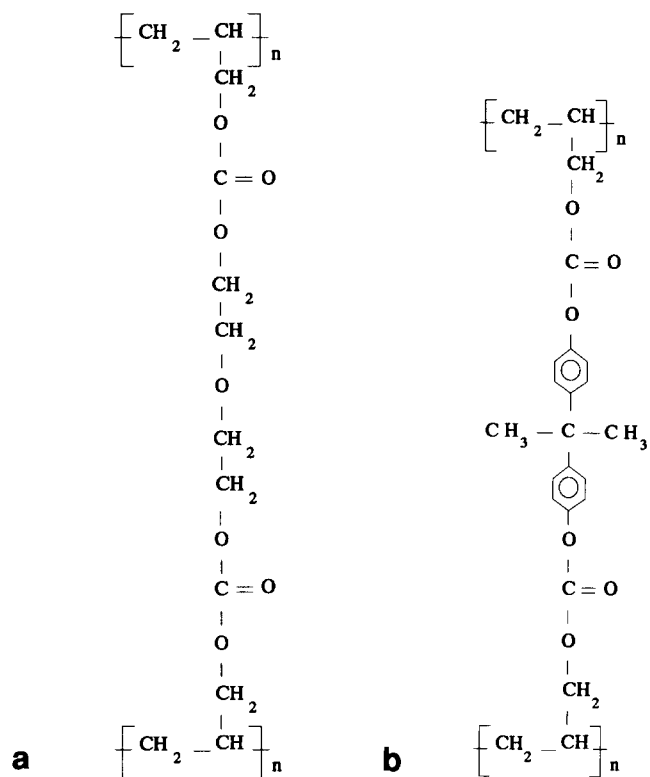


Figure 1 Repeat units of (a) CR39 and (b) HIRI

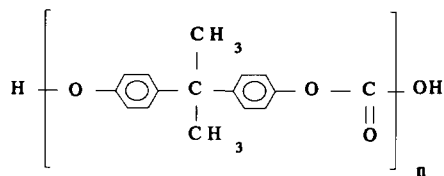


Figure 2 Repeat unit of polycarbonate

RESULTS AND DISCUSSION

Refractive index modifications

The refractive index modifications induced by γ irradiation occur in the entire bulk of the sample. They are achieved by a method based on the principle of Young's slits, described by Figure 3. This interferometric method allows Δn to be determined from:

$$\Delta n = x\lambda/ie$$

where e is the sample thickness, λ is the wavelength used, i is the interfringe and x is the shift of the fringes. The technique has an accuracy of 10^{-4} . In our experiments, the achromatic ray was shifted towards the slit corresponding to the irradiated sample, indicating a positive Δn .

Figure 4 shows the variation of refractive index of CR39 and HIRI as a function of the dose. Δn increases steeply for low doses up to 500 kGy, and a maximum of about 3×10^{-3} can be reached in the range covered by this work.

For ion beam irradiation, refractive index modification occurs on a scale corresponding to the depth penetration of the ion into the material. Table 1 gives the values of the projected path R_p as a function of the energy of H^+ and Li^+ ions for the three polymers.

The refractive index and the index variation depend on the kind of ion, its energy and the fluence (ions cm^{-2}), as shown in Figures 5a and b. A sort of 'mass effect' appears, which leads to a greater increase when the ion mass increases.

The increase of the refractive index induced by ion beam irradiation is one or two orders of magnitude higher than that generated by γ irradiation.

For ion beam irradiation, two kinds of interaction may occur: (1) interaction with electrons, which causes excitation or ionization, leading to link scissions; (2) nuclear scattering. For example, if we consider the linear energy loss of 300 keV protons as a function of depth into CR39 for the two kinds of interaction (electronic and nuclear), as represented in Figure 6, it appears that the energy transfer is due mainly to electron interactions with the material.

Refractive index modification of the CR39 may be caused by proton implantation, which is similar to a doping effect, and/or by the permanent modification of CR39 around the proton path. The first process can be illustrated by Figure 7 representing the distribution of implanted protons, which is localized at the end of the proton path. In these conditions, the refractive index modification would occur at the end of the path and give a buried index profile. The second process corresponds to the fact that the ions gradually lose their energy all along their path; this is represented by the linear energy loss as a function of penetration (Figure 6).

When the refractive index profile is determined experimentally, for example in the case of a 300 keV

proton beam, a monotonically decreasing profile is obtained (Figure 8).

All these considerations lead to the conclusion that the refractive index variation of CR39 irradiated by a proton beam is due mainly to physical and chemical modifications related to the energy transfer of the ions.

Realization of optical waveguides by ion beam

The most obvious application of the local index modification is optical waveguiding. In fact, by ion beam irradiation of CR39, in the energy range of 50–300 keV and with fluences between 10^{13} and 10^{15} ions cm^{-2} , the refractive index variation is adequate ($\geq 5 \times 10^{-3}$) to create a waveguiding layer with thickness corresponding to the penetration depth of the ion (Figure 9).

So, we can produce gradient index waveguides usually characterized by: the number of modes; the effective index (corresponding to a well defined mode); and the loss.

The effective index as a function of fluence for 300 keV protons is represented in Figure 10, which shows the

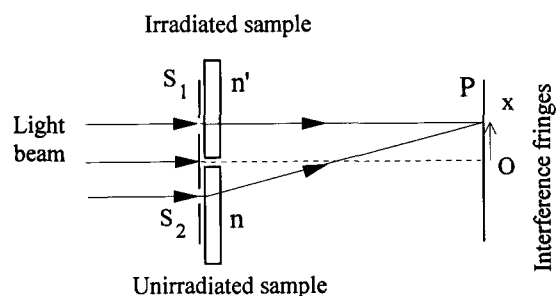


Figure 3 Diagram of the method used to measure Δn in the case of γ irradiation. S_1 , S_2 , Young's slits; P, observation plane

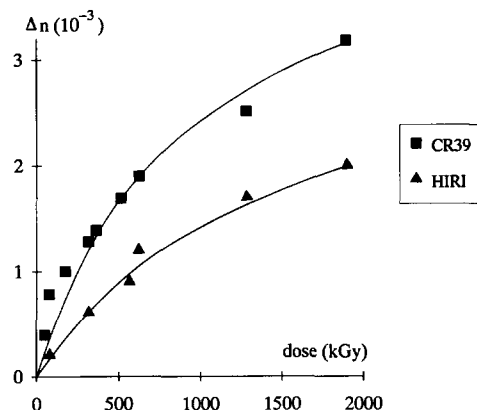


Figure 4 Refractive index variation versus dose for CR39 and HIRI

Table 1 Projected range (R_p) of various ions in CR39, HIRI and polycarbonate (PC) targets

Ion	Energy (keV)	Target	R_p (μm)
$^1H^+$	250	CR39	3.69
$^1H^+$	250	HIRI	3.90
$^1H^+$	250	PC	3.94
$^1H^+$	100	PC	2.07
$^1H^+$	50	PC	1.38
$^7Li^+$	250	CR39	1.72
$^7Li^+$	250	HIRI	1.78
$^7Li^+$	250	PC	1.82

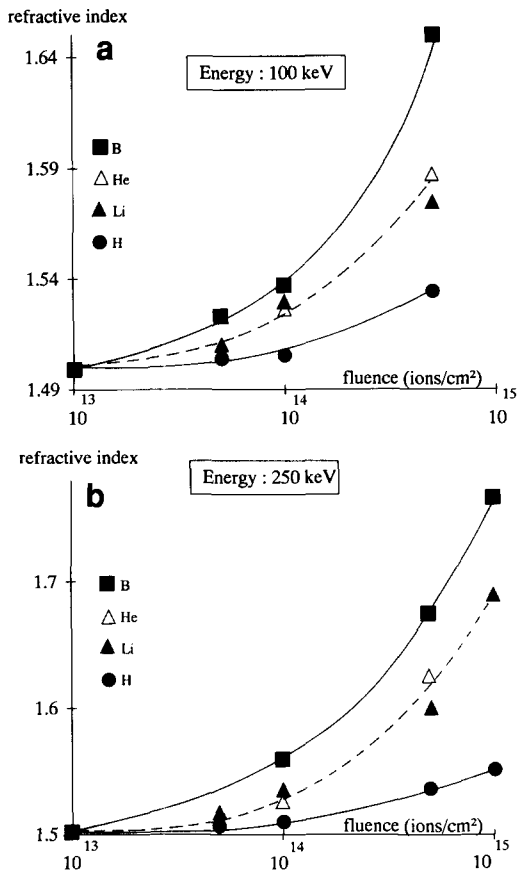


Figure 5 Refractive index variation versus fluence for various ions at 100 keV (a) and 250 keV (b)

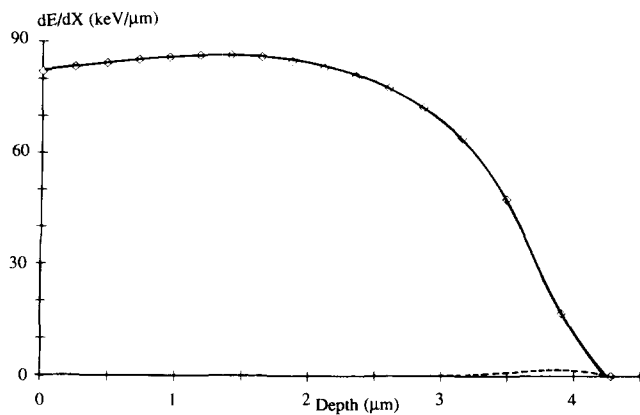


Figure 6 Linear energy transfer as a function of depth (300 keV protons; target, CR39): —, due to electron collisions; ---, due to nuclear collisions

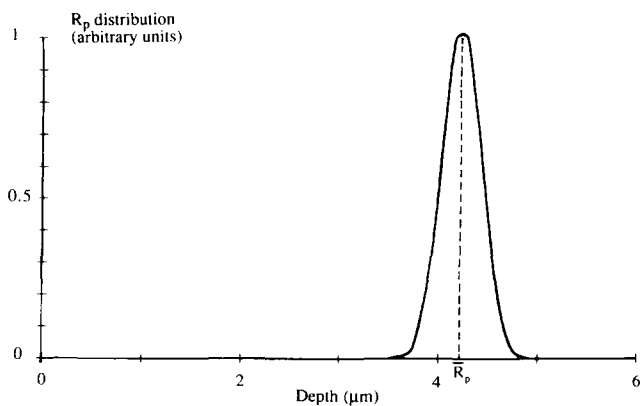


Figure 7 Ion range distribution of a monoenergetic beam of 300 keV protons

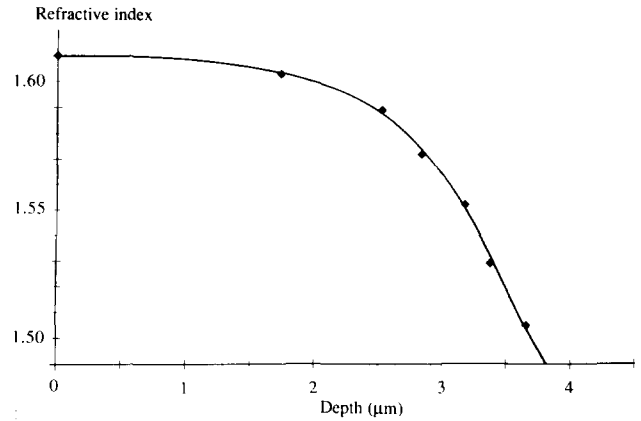


Figure 8 Refractive index profile using 300 keV proton irradiation

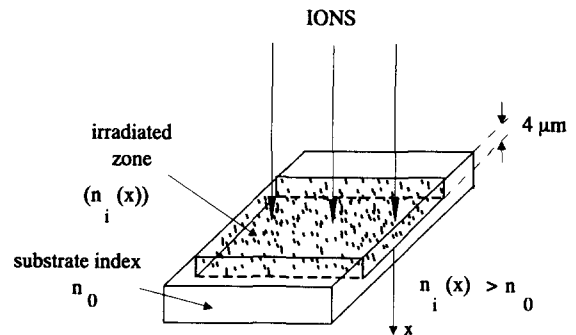


Figure 9 Implanted guide

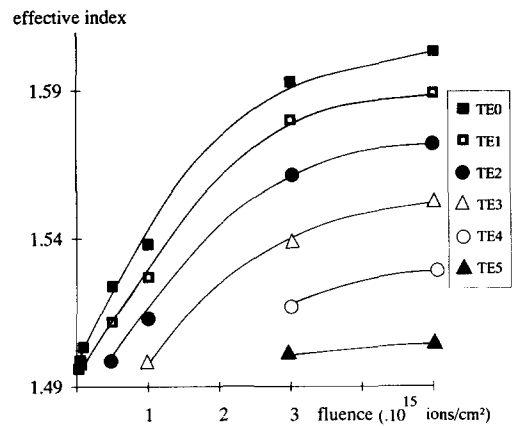


Figure 10 Effective index of the transverse electric modes versus fluence (Φ) for a waveguide in CR39 (300 keV protons). $\Phi = 10^{13}$ and 5×10^{13} ions $\text{cm}^{-2} \rightarrow 1$ mode; $\Phi = 10^{14}$ ions $\text{cm}^{-2} \rightarrow 2$ modes; $\Phi = 5 \times 10^{14}$ ions $\text{cm}^{-2} \rightarrow 3$ modes; $\Phi = 10^{15}$ ions $\text{cm}^{-2} \rightarrow 4$ modes; $\Phi = 3 \times 10^{15}$ and 5×10^{15} ions $\text{cm}^{-2} \rightarrow 6$ modes

number of modes and their effective index increase with fluence.

The losses of the optical waveguides are also related to fluence and energy, as shown in Figure 11. The best performances (2 dB cm^{-1}) were obtained on a CR39 substrate irradiated by protons with energies below 200 keV and fluences below 10^{14} ions cm^{-2} .

We showed that energy and fluence determine the thickness of the waveguiding layer, the refractive index variation and the number of modes, and influence the loss values.

Physical and chemical analyses

In order to increase our understanding of the different processes and to control the characteristics of the

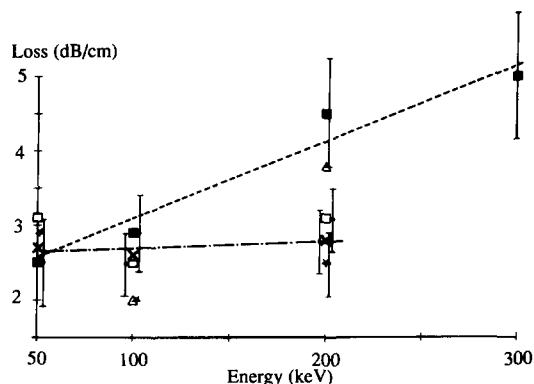


Figure 11 Loss of waveguides in CR39 as a function of the proton energy for various fluences (ions cm^{-2}): ■, 10^{15} ; Δ , 5×10^{14} ; ★, 10^{14} ; ×, 5×10^{13} ; □, 10^{13}

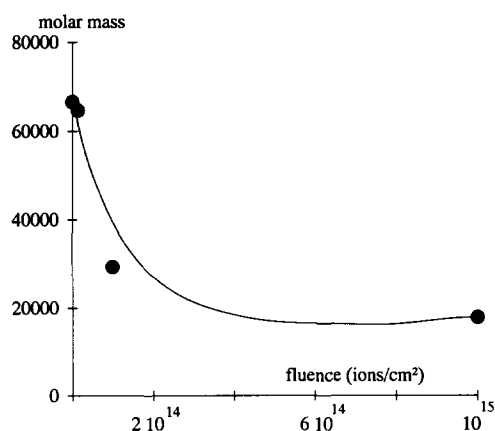


Figure 12 Molar mass distribution versus fluence (100 keV protons; target, polycarbonate)

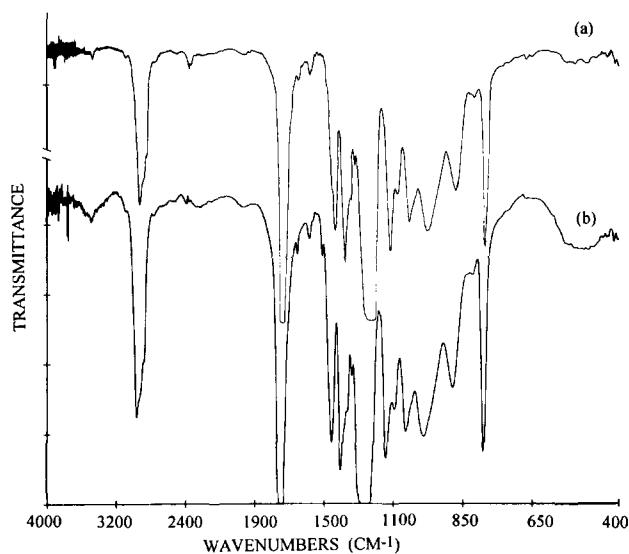


Figure 13 Infra-red absorption spectra of CR39: (a) unirradiated; (b) irradiated (250 keV protons; fluence, 10^{14} ions cm^{-2})

waveguides, a more fundamental study of the polymeric materials was carried out by the use of g.p.c., i.r. spectroscopy⁶ and u.v.-visible spectroscopy.

The molar mass distribution curve obtained by g.p.c. for polycarbonate shows a shift to lower molar mass values when the dose or the fluence increases (Figure 12).

These results show that the main process induced by ion beam or γ irradiation is chain scission, while crosslinking is secondary.

I.r. spectroscopy confirmed that degradation is the essential phenomenon, and also allowed identification of the different absorption bands (Figure 13, Table 2).

A calculation method derived from the Lambert-Beer law is used to determine the amount of chemical bonds responsible for absorption and broken by irradiation. Figure 14 shows plots of the ratio ρ/ρ_0 (concentration of chemical bonds responsible for absorption after and before irradiation) for three chemical groups in CR39, as a function of dose (Figure 14a) and fluence (Figure 14b). From these curves, an order of dissociation appears in both cases: C-O-C, C-H, CH₂ (Figure 14a); C-H, C-O-C, CH₂ (Figure 14b). These different behaviours may be explained by the presence of oxygen during γ irradiation⁷.

Table 2 Absorption bands of CR39

Wavenumber (cm^{-1})	Group
3460	$\nu(\text{O-H})$
3092	$\nu(\text{C-H})$
2960	$\nu(\text{CH}_2)$
1745	$\nu(\text{C=O})$
1650	$\nu(\text{C=C})$
1458	δCH_2
1400	δCH_2
1260	$\nu(\text{C-O})$
1140	$\nu(\text{C-O-C})$
1100	$\nu(\text{C-O-C})$
1028	$\nu(\text{C-O-C})$
961	$\nu(\text{C-O})$ and δCH
878	γCH
791	δCH

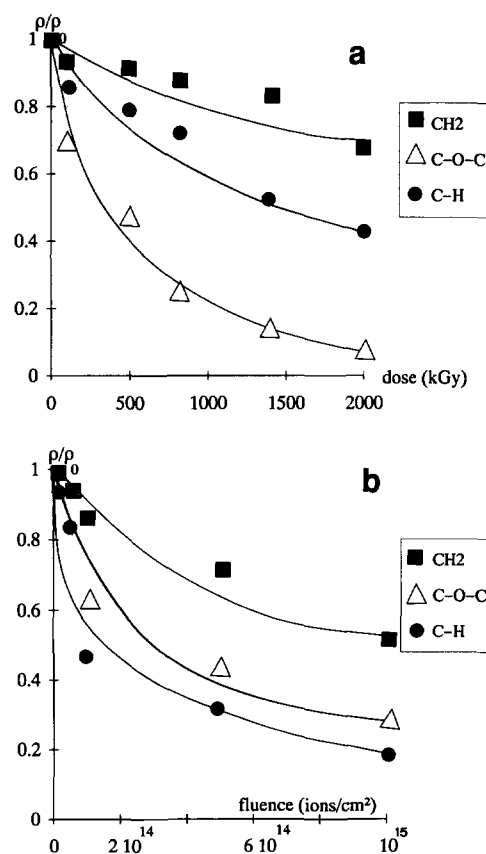


Figure 14 Evolution of three bonds in CR39 with (a) γ dose and (b) fluence (250 keV protons)

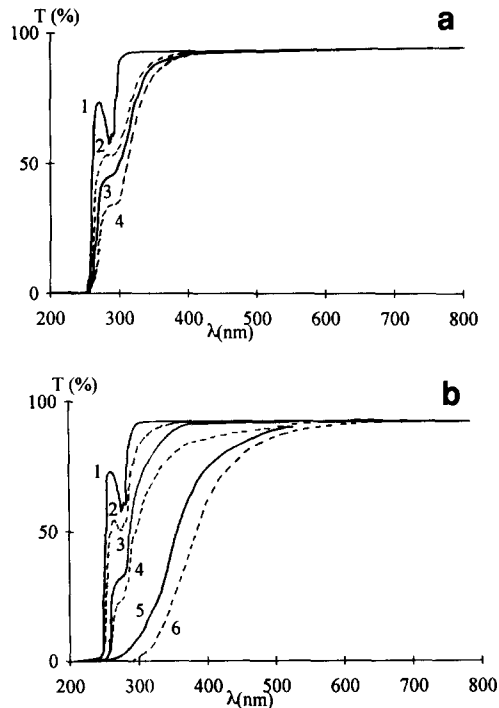


Figure 15 U.v.-visible spectra of CR39. (a) γ irradiation with various doses (D): 1, unirradiated; 2, $D=820$ kGy; 3, $D=1400$ kGy; 4, $D=2000$ kGy. (b) 250 keV protons with various fluences (Φ): 1, unirradiated; 2, $\Phi=10^{13}$ ions cm^{-2} ; 3, $\Phi=5 \times 10^{13}$ ions cm^{-2} ; 4, $\Phi=10^{14}$ ions cm^{-2} ; 5, $\Phi=5 \times 10^{14}$ ions cm^{-2} ; 6, $\Phi=10^{15}$ ions cm^{-2}

The proportion of bond dissociation increases with the dose and the fluence, which is in agreement with other publications^{8,9}, so degradation is essentially the main effect induced by irradiation and is accompanied by an increase in refractive index.

In fact, we have seen that irradiation of CR39 produces drastic changes in the concentration of chemical bonds, but the refractive index variations remain very weak. For example, for a dose of around 500 kGy, the concentration of C–O–C bonds is halved while Δn is about 0.3×10^{-3} .

The evolution of u.v.-visible spectra as a function of irradiation (dose and fluence) is represented in *Figures 15a* and *b*. It is seen from these curves that the 800 nm transmission decreases and that the absorption front shifts to higher wavelengths when the γ dose or fluence increases.

The calculation of the optical gap energy¹⁰:

$$E_g = hc/\lambda$$

where h is the Planck constant and c is the velocity of light in vacuum, as a function of irradiation shows that it decreases with dose or fluence because of an increasing disorder in the material.

Some defects are created in the polymer structure that lead to a distortion of the valence and conduction energy levels and also to an increase in the number of electron transitions.

The u.v.-visible spectra remain unchanged after 1 year or more, indicating that the electron structure modifications can be considered as permanent, and contributing to the increase of absorption and refractive index.

CONCLUSION

This study establishes that optical waveguides can be fabricated in polymers by direct implantation of ions such as H, Li and B, and it also contributes to a better understanding of the structure of irradiated polymers. The refractive index variation depends on the degree of degradation, which is the main process induced by irradiation.

Further study is in progress using electron spin resonance to investigate free radical processes. Another material, prepared by fully controlled polymerization with various concentrations of diisopropyl peroxydicarbonate initiator, is being tested as a waveguide, and exhibits better performances than the first materials used.

REFERENCES

- 1 Bannamane, B., Decossas, J. L., Gagnadre, C. and Vareille, J. C. *Ann. Phys (Paris)* 1989, **14**, 243
- 2 Bannamane, B., Decossas, J. L., Marcou, J. and Vareille, J. C. *SPIE* 1988, **1014**, 132
- 3 Bannamane, B., Decossas, J. L., Gagnadre, C. and Vareille, J. C. *Nucl. Instr. Meth.* 1991, **B62**, 103
- 4 Kulish, J. R., Francke, H., Singh, A., Lessard, R. A. and Knystautas, E. J. *J. Appl. Phys.* 1988, **63**, 2517
- 5 Venkatesen, T., Calcagno, L., Elman, B. S. and Foti, G. in 'Ion Beam Modification of Insulators' (Eds P. Mazzoldi and G. W. Arnold), Elsevier, Amsterdam, 1987, p. 302
- 6 Gagnadre, C., Decossas, J. L. and Vareille, J. C. *Nucl. Instr. Meth.* 1993, **B63**, 48
- 7 Gagnadre, C. *PhD Thesis* Faculté des Sciences, Limoges, 1992
- 8 Chapiro, A. *J. Chim. Phys.* 1956, **53**, 296
- 9 Jenkins, A. D. in 'Polymer Science' (Ed. A. Charlesby), North Holland, Amsterdam, 1972, Ch. 23
- 10 Elman, B. S., Thakur, M. K., Sandman, D. J. and Newkirk, M. A. *J. Appl. Phys.* 1985, **57**, 4996